STATIONARY PROPERTIES OF SUPERCONDUCTING INTERFEROMETERS*

S.J. Lewandowski

Instytut Fizyki Polskiej Akademii Nauk
Al. Lotników 32/46, 02-668 Warszawa, Poland

(Received October 16, 1991; in final form December 6, 1991)

A generalized superconducting interferometer, comprising a parallel arrangement of (lumped) inductances and series (lumped) Josephson junctions is considered. Such a system can be seen as the building block of a simplified model of a high-T_c superconductor with its haphazard distribution of Josephson weak links on grain boundaries and lattice defects. It is shown that the system properties can be self-consistently derived from a properly defined potential energy function, taking account of the energies of the system, its current source and external magnetic field. In particular, by solving a stationary problem for this function relative to conditions of constant current bias and constant magnetic flux applied to the system, the critical current of the interferometer can be determined in function of the applied flux. Stationary phase relations and their impact on other system variables are discussed in detail. The theory is applied to the simplest possible system exhibiting all discussed properties, i.e. an interferometer composed of two junctions in series and one junction in parallel.

PACS numbers: 74.50.+r, 85.25.Dq

1. Introduction

High-T_c materials, both in bulk and thin film form, contain intrinsic Josephson weak links, distributed in a more or less disorderly manner on grain boundaries and crystal lattice defects. In low magnetic fields the junctions can dominate the material properties. Several theoretical models have been proposed to deal with this situation, including single junction and junction array models. For instance, a

*This work was supported by Polish Government Research Grant No. 2 0479 91 01.

single long, tunnel junction has been recently used as a model to explain the critical current dependence on applied magnetic field in a highly textured $YBa_2Cu_3O_7$ thin film [1].

However, many experimental facts indicate that junctions appear in the material rather as clusters, behaving in many respects like parallel arrays (cf. [2]). It can be also reasonably supposed that some of the junctions in the parallel arrays are connected in series. Therefore, the elementary block in any theoretical model of the material in question cannot be reduced beyond a generalized superconducting interferometer, i.e. a parallel arrangement of series connected Josephson junctions and inductances. Theoretical analysis of d.c. properties of such systems, based on a simple model involving ideal, point-like Josephson junctions and lumped inductances, was carried out in Refs. [3, 4]. In particular, it was shown in Ref. [4] that these properties can be derived from the stationary value problem for a properly defined potential energy function.

Section 2 of the present paper gives a concise and systematic exposition of the previous results, highlighting on the relations between stationary superconducting phase differences across the junctions and other variables describing the system state. These relations previously were not subject to a detailed investigation. We show that the behavior of stationary energies and the corresponding stationary values of observable quantities (d.c. current through the system and magnetic flux applied to it) is completely determined by the geometry of the locus of stationary phase points related to the two weakest junctions of the system. In Sec. 3 the theory is applied to a more detailed (numerical) analysis of the simplest possible arrangement involving series junctions, a (2+1)-junction superconducting interferometer. We use this example to discuss the analytical properties of stationary current versus applied flux patterns. Conclusions are presented in Sec. 4.

2. General theory

We consider a superconducting interferometer composed of two parallel arrays of series connected Josephson junctions. The junctions will be treated as lumped elements (point-like devices) and the effects of magnetic field will be accounted for by assuming that the arrays include also series (lumped) inductances. The interferometer is supplied by d.c. current J from an external source and is linked by an externally applied magnetic flux Φ_e. A particular example of the system with only two series junctions is shown in Fig. 1: on the left side we show the possible arrangement of superconducting grains which would give rise to the circuit schematically represented on the right side.

The system is best described in terms of superconducting phase differences φ_{ni} across the junctions, where $n = 1, 2$ refers to the array and $i = 1, 2, \ldots N_n$ to the junction in this array. We need also to introduce the critical currents I_{ni} of the junctions, the currents J_n through each array and the total magnetic flux Φ linking the circuit

$$\Phi = \Phi_e - \Phi_i, \tag{1}$$

where Φ_i denotes the flux induced by current J_n. Using the φ_{ni} variables, the

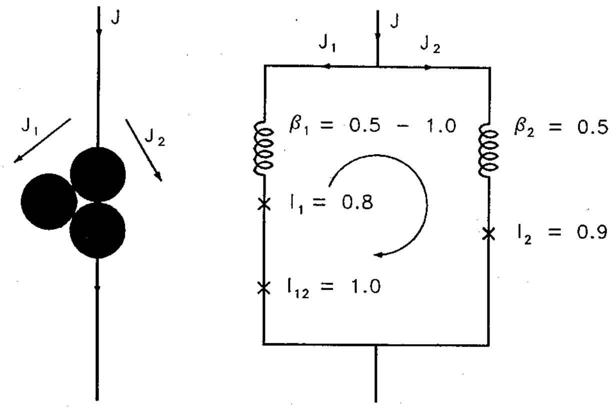

Fig. 1. A (2+1)-junction interferometer created by intrinsic junctions in high-T_c superconductor. Left: dark disks symbolize superconducting grains interconnected by intrinsic Josephson junctions. Right: the equivalent circuit with junctions marked by crosses. The indicated parameter values are used in the numerical calculations discussed in the text. Arrow in the center shows the direction of fluxoid integration path.

potential energy G of the system (current source and external magnetic field included) can be expressed as [4] (cf. also [5]):

$$G = \sum_{ni} I_{ni}(1 - \cos\varphi_{ni}) - \sum_{n} J_n \sigma_n + (\pi/L)\Phi^2, \tag{2}$$

where

$$\sigma_n = \sum_{i=1}^{N_n} \varphi_{ni},$$

and L is the sum of series inductances L_n in each array, $L = L_1 + L_2$. For fluxes we use the units of flux quantum Φ_0, while the inductances are expressed in units of henry/Φ_0.

The first term on the right-hand side of Eq. (2) represents the potential energy of the Josephson junctions, the second is the total energy drawn from the current source in the process of increasing the phase across each junction from 0 to φ_{ni}, and the third is the magnetic energy stored in the system (and in the external field).

Equation (2) is obviously not sufficient to describe the system completely, since it involves the quantities J_n and Φ, so far unrelated, although implicitly assumed to be explicit or implicit functions of the φ_{ni} variables. The missing link can be established by Eq. (1) and by the fluxoid conservation relationship

$$\Phi = (1/2\pi)(\sigma_1 - \sigma_2 + 2\pi q), \tag{3a}$$

where q is an integer, assumed further equal to zero. An alternative choice for a constitutive relation is Eq. (1) and simply the induced flux definition

$$\Phi_i = -J_1 L_1 + J_2 L_2. \tag{3b}$$

Equation (2) can be used to investigate the non-equilibrium behavior of the system, but we limit our interest to the stationary system states. From physical point of view a stationary system state means that the current J drawn from the source and the externally applied flux Φ_e are constant while the energy is extremal. Let us, therefore, examine the extrema of G relative to the conditions

$$\mathrm{d}J = \mathrm{d}(J_1 + J_2) = 0, \qquad \mathrm{d}\Phi_e = 0. \tag{4}$$

The treatment of Φ_e deserves a comment. At a first glance it seems that the second of Eqs. (4) is trivial, since Φ_e is an independent variable (it can eventually depend on time, but time-dependent processes are a priori excluded from the present theory). However, this argument is a fallacy and Φ_e is *not* an independent variable in the considered problem. It has been already observed by Pełka and Zagrodziński [6] that current and magnetic field in a Josephson junction, if specified together with the superconducting phase difference, must be self-consistent.

Observe that Eqs. (4) standing alone can be interpreted as a stationary value problem for J and Φ_e. Another possible interpretation following from the implicit assumption of Kirchhoff's law for currents is that we are dealing with the problem of equilibrium distribution of a given current J into J_1 and J_2 with external flux as a parameter.

We assume initially that all phases φ_{ni} are independent. The currents J_n will then depend on all of these variables

$$J_n = J_n(\varphi_{11}, \ldots, \varphi_{1N_1}, \varphi_{21}, \ldots, \varphi_{2N_2}),$$

and similarly Φ_e, with the reservation that Eqs. (4), in general, allow to eliminate one of the φ_{ni}. Since it is not really important which phase is made dependent, we will denote it by φ^*.

The extrema of G will occur among those points at which all first order derivatives of G are zero. We must have, therefore,

$$G_{'kj} = \sum_{ni} (I_{ni} \sin\varphi_{ni} - J_n)\, \varphi_{ni'kj} - \sum_{ni} J_{n'kj}\varphi_{ni} + (2\pi/L)\Phi\Phi_{'kj}\Big|_{\mathrm{extr}} = 0, \tag{5}$$

where $'kj$ stands for the involved derivative $\frac{\partial}{\partial\varphi_{kj}} + \frac{\partial}{\partial\varphi^*}\frac{\partial\varphi^*}{\partial\varphi_{kj}}$.

Since Eq. (5) must occur for all kj, it is clearly seen that the Josephson equations

$$J_n = I_{ni} \sin\varphi_{ni}, \qquad n = 1, 2, \qquad i = 1, 2, \ldots N_n, \tag{6}$$

constitute a necessary condition for the existence of an energy extremum. It suffices that these equations are satisfied only at the extremum, but for later use we will assume now that they constitute an additional constraint imposed on the system and are differentiable.

Taking into account Eqs. (6) and (4), Eq. (5) is reduced to

$$G_{'kj}\big|_{\mathrm{extr}} = (-\sigma_1 + \sigma_2)J_{1'kj} - (2\pi/L)\Phi\Phi_{i'kj} = 0. \tag{7}$$

It is seen from this result that if the constraint $\mathrm{d}\Phi_e = 0$, Eqs. (4), are replaced by $\mathrm{d}\Phi = 0$, seemingly in the spirit of fluxoid conservation, then the corresponding relative extremum occurs only at $\Phi = 0$. With our constraint, it is easily shown [4] that if one of Eqs. (3a) and (3b) is assumed to be generally valid, then the second one is obtained as a sufficient condition for the existence of energy extremum.

In proof, let us asume that the fluxoid relationship Eq. (3a) is a constitutive (differentiable) relation for the functions involved in Eq. (2). Equation (7) yields then

$$(\sigma_1 - \sigma_2)\,[-J_{1'kj} - (1/L)\Phi_{i'kj}] = 0.$$

Clearly, the extremum is either coincident with the minimum of the parabolic magnetic energy term

$$\Phi \propto (\sigma_1 - \sigma_2) = 0,$$

or it is a local extremum, which requires

$$(1/2\pi)(\sigma_1 - \sigma_2)_{'kj} = -\Phi_{i'kj} = LJ_{1,kj} = (L_1 J_1 - L_2 J_2)_{'kj},$$

i.e. as a consequence of the initial assumption we obtain the differential form of Eq. (3b). We note also the trivial conditions $J_{1'kj} = 0$ and $J_{2'kj} = 0$, corresponding to current expulsion from one of the parallel interferometer arms, i.e. to a situation in which magnetic interaction vanishes (at least within the scope of the present theory).

Let us assume now that it is Eq. (3b) which takes on the role of a definition. Equation (7) is then

$$(-\sigma_1 + \sigma_2)J_{1'kj} - (2\pi/L)\Phi(-L_1 J_{1'kj} + L_2 J_{2,kj}) =$$

$$= (-\sigma_1 + \sigma_2 + 2\pi\Phi)J_{1,kj} = 0,$$

i.e. we obtain Eq. (3a) for $q = 0$. This complementarity of the fluxoid and induced flux is an unexpected but æstethically pleasing development of the theory. It should be pointed out that this result relies heavily on consistent usage of signs in Eqs. (1) and (2), determined primarily by the orientation of the fluxoid integration path with respect to J_n.

In order to fix attention, let us return to the assumption of constitutive character of Eq. (3a) and let us proceed with effective solution of the considered problem. We need to conduct first some ordering operations. Equations (6) are clearly redundant and the number of independent variables φ_{ni} can be reduced to two. Let the indices ni be ordered so that $I_{ni} \le I_{nj}$ for $i < j$ and let $I_{11} \le I_{21}$. The indices $n1$ will be further abbreviated to n, in anticipation of the special role the weakest junction in each array is going to play. We introduce also the notation $a = I_1/I_2$, $a_{ni} = I_n/I_{ni}$. Then Eqs. (6) for $n = 1, 2$ and $i \ge 2$ are rewritten as

$$\varphi_{ni} \equiv \varphi_{ni}^{(m)} = (-1)^{m_{ni}}\varphi_{ni}^{(0)} + m_{ni}\pi, \qquad i \ge 2, \tag{8}$$

where m_{ni} is an integer and $\varphi_{ni}^{(0)}$ denotes the principal branch of $\arcsin(a_{ni}\sin\varphi_n)$, i.e. $-\pi/2 \le \varphi_{ni}^{(0)} \le \pi/2$. Observe that for $a_{ni} < 1$, the ranges of $\varphi_{ni}^{(m)}$ and $\varphi_{ni}^{(m+1)}$ are separated by a phase gap of width [3]:

$$2\Psi_{ni} = 2\arccos a_{ni}, \qquad 0 \le \Psi_{ni} \le \pi/2,$$

which cannot be entered without exceeding the critical current I_n.

The system is now completely described by the phase differences φ_1 and φ_2 across the weakest junction in each array and by the "state vector" $\langle\widehat{m}\rangle = \langle\widehat{m}_1, \widehat{m}_2\rangle$ with $N_1 + N_2 - 2$ components $\langle\widehat{m}\rangle_{ni} = m_{ni}$ *. Moreover, the remaining two Eqs. (6) and Eq. (3a) relate φ_1 and φ_2 to each other. Choosing φ_1, the phase of the weakest junction of the system, as the independent variable, applying the method of implicit differentiation to Eqs. (4) and using the Josephson equations as an additional constraint, we obtain after some manipulations [3] the necessary condition for a phase point (φ_1, φ_2) to be stationary

$$\frac{1}{\cos\varphi_1} + a\frac{1}{\cos\varphi_2} + \beta_1^{\langle\widehat{m}\rangle}(\varphi_1) + a\beta_2^{\langle\widehat{m}\rangle}(\varphi_2) = 0, \tag{9}$$

where

$$\beta_n^{\langle\widehat{m}\rangle}(\varphi_n) = -\beta_n + \sum_{i=2}^{N_n} \frac{(-1)^{m_{ni}} a_{ni}}{\sqrt{1 - a_{ni}^2 \sin^2\varphi_n}},$$

and $\beta_n = 2\pi L_n I_n$. Equation (9) must be solved numerically for $\varphi_2^{\langle\widehat{m}\rangle}(\varphi_1)$ [or $\varphi_1^{\langle\widehat{m}\rangle}(\varphi_2)$], the locus of the stationary points (φ_1, φ_2), dependent on the state vector $\langle\widehat{m}\rangle$ assigned to the system.

In general, the solution does not exist for an arbitrary value of φ_1 or φ_2. This can be easily shown in the case of a two-junction interferometer. Then $\beta_n^{\langle\widehat{m}\rangle} = -\beta_n$ and Eq. (9) in $x = (\cos\varphi_1)^{-1}$ and $y = (\cos\varphi_2)^{-1}$ coordinates is a straight line

$$x + ay - \alpha = 0, \qquad \alpha = \beta_1 + a\beta_2,$$

everywhere except inside the region bound by the lines $|x| = 1$ and $|y| = 1$. The importance of the parameter α in the analysis of a two-junction interferometer was first realized by Fulton, Dunkleberger and Dynes [8]. Intersection points of the solution line with the region boundaries define the forbidden ranges of φ_1 and φ_2, which are void only for $a = 1$ and $\beta_1 = \beta_2 = 0$. In the general case of nonlinear $\beta_n^{\langle\widehat{m}\rangle}$ the straight solution lines are replaced by curves, but the overall picture is not greatly changed, as is demonstrated in Fig. 2 for the particular case of the system shown in Fig. 1, i.e. $N_1 = 2$, $N_2 = 1$, $I_1 = 0.8$, $I_{12} = 1.0$, $I_2 = 0.9$, $\beta_2 = 0.5$, and two values of $\beta_1 = 0.5, 1.0$.

From the above observations it can be deduced that the plots $\varphi_2^{\langle\widehat{m}\rangle}(\varphi_1)$ form on the φ_1, φ_2-plane closed, periodically spaced loops (in direct analogy to fluxon vortices), separated by regions where stationary solutions cannot exist. In Fig. 3 we show the phase patterns resulting from the plots of Fig. 2. The existence of such loops or phase vortices was recognized in the two-junction case by Tsang and Van Duzer [9].

The appearance of forbidden gaps in the ranges of *stationary* phases $\varphi_n^{\langle\widehat{m}\rangle}$ is not related to the gaps in φ_{ni}, introduced by Eq. (8). The latter cannot be

*Asigning a phase state to a specific system, we will use the notation $\langle\widehat{m}\rangle_-$, the subscript "$-$" to remind of the minus sign in Eq. (1) (earlier usage was different, cf. [3, 4]).

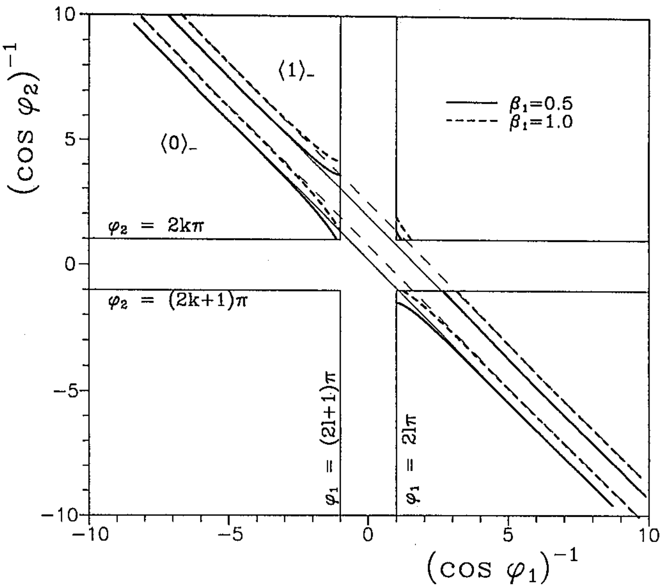

Fig. 2. Plots of inverse cosines of stationary phases for the (2+1)-junction interferometer shown in Fig. 1 ($N_1 = 2$, $N_2 = 1$, $I_1 = 0.8$, $I_{12} = 1.0$, $I_2 = 0.9$, $\beta_2 = 0.5$), and two values of β_1: 0.5 (solid lines) and 1.0 (dashed lines). Lower plots represent the even $\langle 0\rangle_-$ phase state, and the upper ones — the odd $\langle -1\rangle_-$ state.

crossed without current being first expelled from the relevant junction array while the former can be bridged by any non-equilibrium process.

Assuming that the Josephson equations, Eq. (6), and fluxoid conservation relationship, Eq. (3a), are always satisfied, while the induced flux definition, Eq. (3b), occurs only at the energy extremum, we are essentially considering a situation in which the superconducting phases adjust immediately to the instantaneous values of J_1, J_2 and Φ but these values lag behind the changes in Φ_e. Under these assumptions it is also possible to calculate the second derivative $G''\langle\widehat{m}\rangle$ of $G^{\langle\widehat{m}\rangle}$ with respect to φ_1. Differentiating Eq. (5) we arrive after some manipulations at the result [4]:

$$\frac{LG''\langle\widehat{m}\rangle}{\cos^2\varphi_1} = \left(\eta_1^2\tan\varphi_1 - a^2\eta_2^2\tan\varphi_2^{\langle\widehat{m}\rangle}\right)\Phi^{\langle\widehat{m}\rangle}, \tag{10}$$

where

$$\eta_n^2 = \sum_i \frac{a_{ni}^2}{\cos^2\varphi_{ni}} = \sum_i \frac{a_{ni}^2}{1 - a_{ni}^2\sin^2\varphi_n},$$

and $\Phi^{\langle\widehat{m}\rangle}$ denotes the flux calculated from Eqs. (3a), (8), and (9). By calculating the sign of this expression it is possible to identify the stationary points as energy minima, maxima, and inflection points.

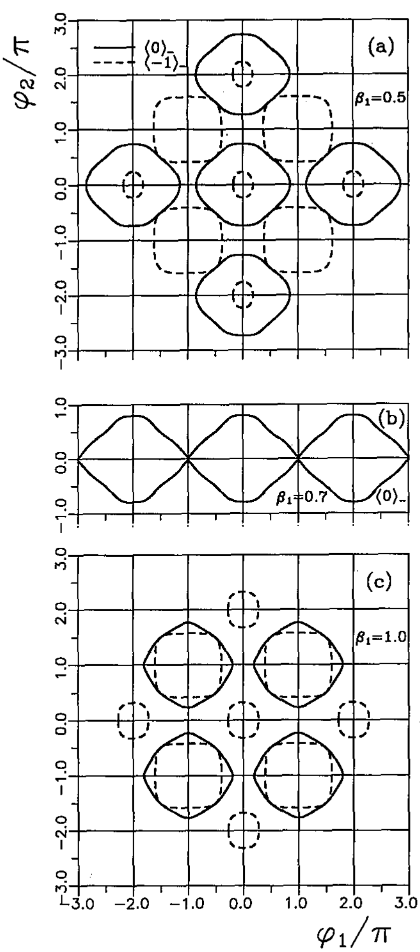

Fig. 3. Stationary phase plots resulting from the solution lines of Fig. 2; (a) $\beta_1 = 0.5$, (b) $\beta_1 = 0.7$, (c) $\beta_1 = 1.0$.

3. Stationary states

Some insights into the system's behavior can be gained from numerical solutions of Eq. (9). Obviously, only a limited number of situations can be reviewed in this manner. We have chosen the simplest possible example, that of a (2+1)-junction interferometer, whose state vector has only one component. Circuit parameters are those indicated in Fig. 1.

The key to understanding the stationary properties of the system is in the inverse cosine plots of Fig. 2 and in the resultant phase plots, shown in Fig. 3. As seen, the loops (vortices) of the stationary phase points $\varphi_2^{\langle\widehat{m}\rangle}(\varphi_1)$ are covering more or less tightly the phase plane and their centers form a square lattice with lattice constant of 2π. System properties are determined by the "unit cell" of this lattice with lattice points at the corners and in the center of a square with 2π sides. The gaps between phase vortices indicate, as already observed, the regions where stationary solutions do not exist. Gap magnitude clearly depends on the β_n's and system state. As a consequence of these gaps, the stationary phases can change continuously only on a vortex line and jump discontinuously from vortex to vortex. An interesting exception from this rule, marking the beginning of a dramatic change in the unit cell of $\langle 0\rangle_-$ state, is shown in Fig. 2b for a particular value of $\beta_1 = 0.7$.

The existence of flat phase fronts, where the derivative of one phase with respect to the other tends to infinity, may be related to the mechanism causing the vortex-to-vortex transitions.

It is clear from the preceding section that a stationary value of current, given by Eqs. (6) and Kirchhoff's law must correspond to each stationary phase point $(\varphi_1^{\langle\widehat{m}\rangle}, \varphi_2^{\langle\widehat{m}\rangle})$

$$J^{\langle\widehat{m}\rangle} = I_1 \sin\varphi_1^{\langle\widehat{m}\rangle} + I_2 \sin\varphi_2^{\langle\widehat{m}\rangle}. \tag{11}$$

Similarly, one can calculate from Eqs. (3) and (8) the corresponding stationary value of externally applied flux

$$\Phi_e^{\langle\widehat{m}\rangle} = \frac{1}{2\pi}\left[\sigma_1^{\langle\widehat{m}\rangle} - \sigma_2^{\langle\widehat{m}\rangle} - \beta_1 \sin\varphi_1^{\langle\widehat{m}\rangle} + \beta_2 \sin\varphi_2^{\langle\widehat{m}\rangle}\right], \tag{12}$$

where $\sigma_n^{\langle\widehat{m}\rangle}$ denotes the sum of stationary phases in the relevant junction array. Finally, from the above relations and Eq. (2) the stationary value of energy $G^{\langle\widehat{m}\rangle}$ can be evaluated. The next obvious step following these transformations is to replace the phase representation by a more convenient one, in which e.g. $J^{\langle\widehat{m}\rangle}$ and $G^{\langle\widehat{m}\rangle}$ are considered to be functions of $\Phi_e^{\langle\widehat{m}\rangle}$. It might be said that from an upside down position, in which the parameters like total current and externally applied flux — instinctively believed to be independent variables — were treated as being out of control, we are now gradually working to a more normal point of view. Such an interpretation, however, might be misleading. The theory provides only the means to check whether the experimentally applied J and Φ_e are a stationary pair $(J^{\langle\widehat{m}\rangle}, \Phi_e^{\langle\widehat{m}\rangle})$.

Suitably normalized graphs of the functions $J^{\langle\widehat{m}\rangle}(\Phi_e)$ and $G^{\langle\widehat{m}\rangle}(\Phi_e)$ (we drop the unnecessary superscript $\langle\widehat{m}\rangle$ from Φ_e designation) are shown in Fig. 4 for $\langle\widehat{m}\rangle = \langle 0\rangle_-$ (solid lines) and $\langle\widehat{m}\rangle = \langle -1\rangle_-$ (dashed lines). Only negative values of $J^{\langle\widehat{m}\rangle}(\Phi_e)$, normalized to $I_{\max} = I_1 + I_2$, cf. Eq. (11), are plotted. Full current plots can be visualized by taking into account their C_2 point symmetry (see also Fig. 5). Energy is scaled by a factor of $L/(\pi I_{\max})$, i.e. taking into account that L was defined as $L \propto L/\Phi_0$, it is normalized to Josephson coupling energy of a junction with critical current $I_c = I_{\max}$ and multiplied by true total inductance of the interferometer loop. The reference level of energy was set equal to $G^{\langle 0\rangle}(0)$ for $\beta_1 = 0.5$. The linewidth used to plot the graphs carries the additional information about the sign of the second-order derivative of $G^{\langle\widehat{m}\rangle}$ with respect to φ_1, calculated

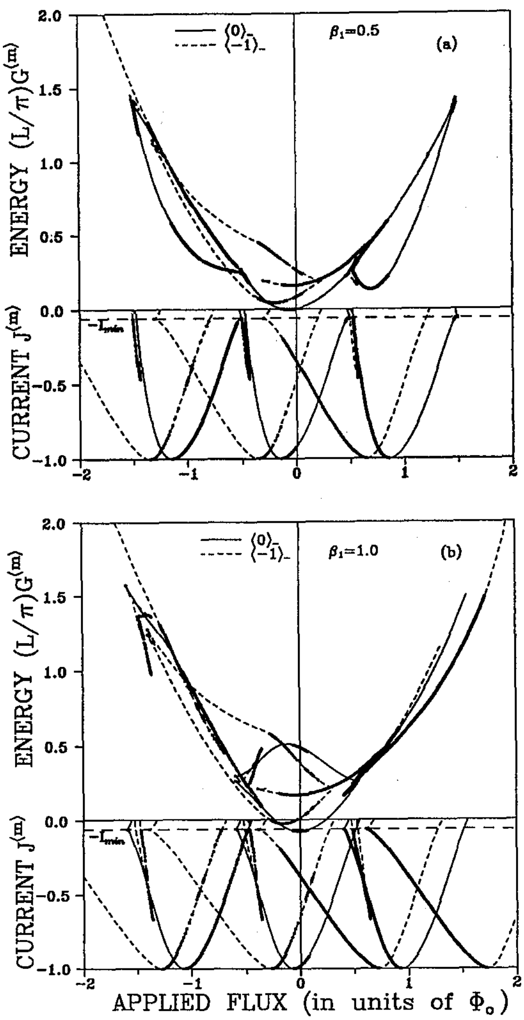

Fig. 4. Stationary energy function $(L/\pi)G^{\langle\widehat{m}\rangle}$ (upper part of each drawing) and stationary current $J^{\langle\widehat{m}\rangle}$ (lower part of each drawing) in function of externally applied magnetic flux Φ_e for $\langle\widehat{m}\rangle = \langle 0\rangle$ (solid lines) and $\langle\widehat{m}\rangle = \langle -1\rangle$ (dashed lines) corresponding to the phase plots of Fig. 3. Both $G^{\langle\widehat{m}\rangle}$ and $J^{\langle\widehat{m}\rangle}$ are normalized to $I_{\max} = I_1 + I_2$; only negative values of the current are shown. Thick lines are used to draw stable solution branches corresponding to local minima of energy; (a) $\beta_1 = 0.5$, (b) $\beta_1 = 1.0$.

from Eq. (10): thick lines correspond to positive sign or local minimum of energy (in the phase space), thin lines — to negative sign or local maximum of energy. Thick lines denote thus the stationary system states which are stable with respect to phase changes. Stable and unstable solution branches appear to succeed each other

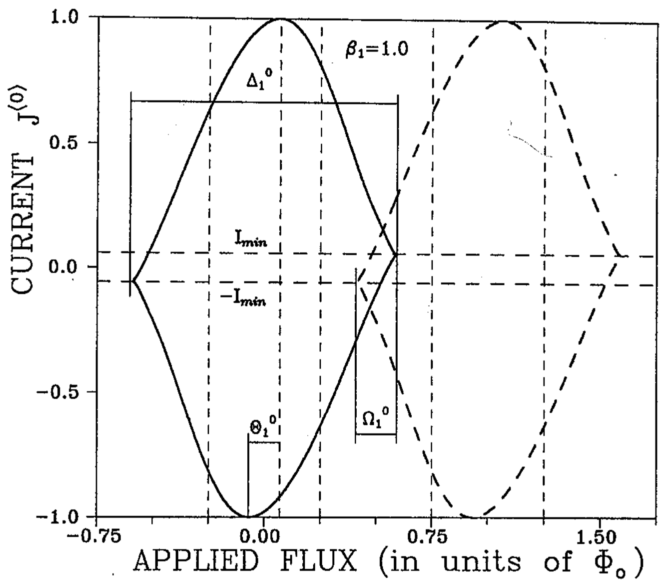

Fig. 5. Full current pattern ($\langle\widehat{m}\rangle = \langle 0\rangle_-$ and $\beta_1 = 1$) and its geometry. Dashed pattern shows the overlap of adjoining flux ranges.

at haphazard. Interpretation of these data might be helped by the observation that the energy surface corresponding to each phase state, stretched over the φ_1, φ_2-plane is composed of a series of twisted Riemann sheets. The contour of stationary energies on any sheet is continuous and its projection on the plane is just a phase vortex. As it has been already explained, we are using another, one-dimensional projection in which a pair of φ_1, φ_2 coordinates is replaced by a single Φ_e value.

The plots in Fig. 4 look quite complicated, but their general structure is easily explained by the underlying lattice of stationary phase vortices. Lattice points, i.e. vortex centers, are located at $(p\pi, q\pi)$, where p, q are integers of the same parity (Fig. 3). Let us consider Φ_e range corresponding to a given vortex. Let Φ_e be minimal at a phase point with coordinates $\varphi_{1(1)} = q\pi - \delta_1$ and $\varphi_{2(1)} = r\pi + \delta_2$, where δ_1 and δ_2 are as yet undetermined. From the vortex symmetry it follows that the point with coordinates $\varphi_{1(2)} = q\pi + \delta_1$ and $\varphi_{2(2)} = r\pi - \delta_2$ is also on the vortex line and the corresponding Φ_e value is maximal. Equation (12) yields then for the flux range in the particular case of the system shown in Fig. 4:

$$2\pi\Phi_{e\,qr} = (q - r + m)\pi$$

$$\mp \left\{\delta_1 + \delta_2 \pm \left[(-1)^m \varphi_{12}^0(\delta_1) - (\beta_1 \sin\delta_1 + \beta_2 \sin\delta_2)\right]\right\},$$

where the upper sign inside the curly braces refers to q, r even, the lower sign to q, r odd, and m, φ_{12}^0 have the same meaning as in Eq. (8), in particular $\varphi_{12}^{(0)}(\delta_1) = \arcsin(a_{12} \sin\delta_1)$.

The expression for $\Phi_{e_{qr}}$ can be easily extended to cover the general case: the $(m = m_{ni})$-dependent terms must be summed up over ni, $i \geq 2$. We will not use this extended version but will make some cosmetic changes in its present form. Instead of the π-multiples q, r let us number the vortices by q', r' introduced by $q = 2q'$, $r = 2r'$ for lattice parity $p = 0$ or $q = 2q' + 1$, $r = 2r' + 1$ for $p = 1$. We will introduce also explicitly the width $\Delta_p^{(\widehat{m})}$ (cf. Fig. 5) of the interval occupied by $\Phi_{e\ qr} = \Phi_{e\ q'r',p}$. Then

$$\Phi_{e\ q'r',p} = q' - r' + \frac{m}{2} \mp \frac{1}{2}\Delta_p^{(\widehat{m})}, \tag{13a}$$

and

$$\Delta_p^{(\widehat{m})} = \frac{1}{\pi}\left\{\delta_1 + \delta_2 + (-1)^p \left[(-1)^m \varphi_{12}^{\circ}(\delta_1) - (\beta_1 \sin\delta_1 + \beta_2 \sin\delta_2)\right]\right\}. \tag{13b}$$

As seen, the ranges of Φ_e for m-even states are centered around integer multiples of Φ_0, while for m-odd states the center is shifted for $\frac{1}{2}\Phi_0$. Next it can be observed that $\Phi_{e\ q'r'}$ is a linear function of one of its indices if the other one is kept constant, i.e. if the phase vortex lattice is run over in horizontal or vertical direction. However, if the lattice is traversed in any (constant) diagonal direction, the flux range is always the same.

Now, $\Phi_{e\ q'r'}$ is the domain of $J^{(\widehat{m})}(\Phi_e)$ and $G^{(\widehat{m})}(\Phi_e)$, both limited to the single relevant phase vortex. From Eq. (11) it is evident that the closed vortex line must be transformed into a closed current pattern and from the same equation and Eqs. (13) it is obvious that this pattern will be periodically repeated every Φ_0, on condition that vortex-to-vortex transitions are along horizontal or vertical lines on the φ_1, φ_2 plane. That is exactly what would be seen in Fig. 4 if the current graphs were completed by positive values: each would form a closed pattern resembling in shape a distorted ace of diamonds (cf. [3]).

$G^{(\widehat{m})}$ is not a periodic function of the phases and each phase vortex must have a unique energetical signature. However, energy contains periodic terms and it can be shown that the graph $G^{(\widehat{m})}(\Phi_{e\ q'r'})$ forms also a closed loop, composed of two twisted branches (as in figure 8 or ∞), which correspond to positive and negative current directions, the twist occurring between flux points corresponding to $J^{(\widehat{m})} = \pm I_{\max}$. This is *not* shown in Fig. 4, where in order not to clutter further the drawing only energies corresponding to negative currents are plotted. In fact, we are applying a convention in which only a diagonally cut slice of each vortex is used. The horizontal and vertical movements across the vortex lattice ($\langle\widehat{m}\rangle$ fixed) in this convention are equivalent to monotonic changes of φ_1 and φ_2, respectively. Energy looping, which can be discerned in Fig. 4, is caused by the already discussed appearance of identical flux ranges for $q' = q'_0$, $r' = r'_0$ and $q' = q'_0 + 1$, $r' = r'_0 + 1$.

Not much more can be said about the general properties of the graphs in Fig. 3 without some attempt at determining δ_1 and δ_2 in Eq. (13b). Analytically it might be quite difficult, but a heuristic approach is suggested by the current graphs. A current pattern must span the entire width of $\Phi_{e_{q',r'}}$. Figure 4 shows that the flux span of the wide current patterns extends from the flux at which $J^{(\widehat{m})} = -I_{\min}$ to the flux at which $J^{(\widehat{m})} = +I_{\min}$, where $I_{\min} = I_1 - I_2$

(the designation used in d.c. SQUID theory, cf. [7]). On the other hand, in deriving Eq. (13b) we have assumed that the flux range limits correspond to the phase points $\varphi_{1(1,2)} = q\pi \mp \delta_1$ and $\varphi_{2(1,2)} = r\pi \pm \delta_2$. It follows immediately that

$$I_1 \sin\delta_1 - I_2 \sin\delta_2 = I_1 - I_2 \tag{14}$$

or $\delta_1 = \delta_2 = \pi/2$. (Some objections may be raised at this point. For the points $\varphi_{1(1,2)}$ and $\varphi_{2(1,2)}$ to be on the vortex line, δ_1 and δ_2 must satisfy Eq. (9), which has a singularity for $\cos\varphi_{1,2} = 0$. Strictly speaking, a limit should be taken on approaching this singularity, but we consider it is sufficient that numerical solutions exemplified in Fig. 3 confirm our choice of δ_1 and δ_2.) With this result Eq. (13b) simplifies to

$$\Delta_p^{(\widehat{m})} = 1 + \frac{(-1)^p}{\pi}[(-1)^m \Psi_{12} - \beta]\,, \tag{15}$$

where Ψ_{12} is the phase gap of junction "12", defined by Eq. (8), and $\beta = \beta_1 + \beta_2$. It is seen immediately that the overlap of two consecutive flux ranges, $\Omega_p^{(\widehat{m})}$, can be expressed as

$$\Omega_p^{(\widehat{m})} = \Delta_p^{(\widehat{m})} - 1 = \frac{(-1)^p}{\pi}[(-1)^m \Psi_{12} - \beta]\,.$$

Equation (15) is valid for the wide current patterns of Fig. 4, i.e. for large phase vortices of Fig. 3. Inspection of narrow $J^{(-1)}$ graphs in Fig. 4, corresponding to the small vortices in Fig. 3, shows that instead of Eq. (14) one should use the condition

$$I_1 \sin\delta_{01} - I_2 \sin\delta_{02} = 0, \tag{16}$$

which together with Eq. (9) allows to determine $\delta_{02} \le \delta_{01} \le \pi/2$.

Equation (14) suggests that another characteristic flux range can be introduced and easily determined: the distance $\Theta_p^{(\widehat{m})}$ between the maxima of $|J^{(\widehat{m})}| = I_{\max}$, which is a measure of current pattern skew (Fig. 5). This is clearly the difference between fluxes corresponding to the phase points ($\varphi_{1(3)} = q\pi + \delta_1$, $\varphi_{2(3)} = r\pi + \delta_2$) and ($\varphi_{1(4)} = q\pi - \delta_1$, $\varphi_{2(4)} = r\pi - \delta_2$), and in order to determine $\Theta_p^{(\widehat{m})}$ it suffices to replace δ_2 in Eq. (13b) by $-\delta_2$. In this manner we obtain for the wide current patterns

$$\Theta_p^{(\widehat{m})} = \frac{(-1)^p}{\pi}[(-1)^m \Psi_{12} - \beta_1 + \beta_2]\,. \tag{17}$$

It should be observed that in Eqs. (15) and (17) the contribution from the series junction "12" is in the same class as the contributions from inductances L_1 and L_2. This is not surprising, since series junctions constitute, in fact, an additional nonlinear inductive load on the system. Let us also note that the listed equations can be used for approximate, linearized construction of the stationary current and energy vs. external flux patterns, what may be useful in high-T$_c$ d.c. (multi-junction) SQUID design. Our results for flux ranges are a generalization of the results obtained by Tsang and Van Duzer [8] for the particular case of a 2-junction interferometer.

A very important question must be asked now: is the topological sum of all flux ranges, given by Eq. (13a) for fixed $\langle\widehat{m}\rangle$, equal to the set of all real numbers? In other words, we are asking whether for any given Φ_e value there exists always a stationary current $J^{\langle\widehat{m}\rangle}(\Phi_e)$. The answer appears to be positive even if the inductive term in square brackets in Eq. (15) becomes negative, but once again the analytical proof is missing. We are left to numerical experiments, which reveal a very interesting mechanism imbedded in Eq. (9): the product of the inductive term and $(-1)^p$ is always non-negative, hence $\Delta_p^{\langle\widehat{m}\rangle} \geq 0$. Whenever the inductive term becomes negative, the phase vortex lattice points are switched to odd multiples of π. How this mechanism takes hold is illustrated in Fig. 3 for $\langle\widehat{m}\rangle = \langle 0\rangle_-$, where for $\beta_1 = 0.5$ the inductive term is positive and $p = 0$ (Fig. 3a), while for $\beta_1 = 1.0$ it becomes negative and $p = 1$ (Fig. 3c); the intermediate situation $\Delta_p^{\langle\widehat{m}\rangle} \approx 0$, shown in Fig. 3b, occurs for $\beta_1 = 0.7$. Similarly, phase vortices of a 2-junction interferometer for which the inductive term must be always ≤ 0 are located at odd multiples of π, i.e. $p = 1$.

From the preceding discussion it follows that the $\Delta_p^{\langle\widehat{m}\rangle}$ interval is shared by the neighboring external flux ranges of the same phase state, *eo ipso* by the neighboring current and energy patterns. However, the lower limit of this range corresponds to $J^{\langle\widehat{m}\rangle} = -I_{\min}$, while the higher limit to $J^{\langle\widehat{m}\rangle} = I_{min}$. It means that a vortex-to-vortex transition involves an abrupt redistribution of currents J_1 and J_2 (cf. also [8]). Such transition is clearly a dynamic process and its particulars would depend on dynamic properties of the system. The positioning of the series junction(s) on the edge of phase gap must also favor in the discussed flux interval the initialization of transitions between different phase states. Even without such transitions the overlapping flux ranges corresponding to different currents (and energies) indicate hysteretical behavior of the system.

The transport properties of the system are determined by its *critical current* $J_{\max}(\Phi_e)$, defined as the maximal d.c. current which can be drawn from the current source at a given Φ_e without driving the system to the resistive state. Since $J^{\langle\widehat{m}\rangle}$ are by definition extremal currents, we can determine the critical current from the relation

$$|J_{\max}(\Phi_e)| = \max_{\langle\widehat{m}\rangle} \left|J^{\langle\widehat{m}\rangle}(\Phi_e)\right|, \tag{18}$$

i.e. assume that $J_{\max}(\Phi_e)$ is the envelope of all $J^{\langle\widehat{m}\rangle}(\Phi_e)$. The relations between stationary currents and fluxes are completely symmetric and we could determine as well critical flux $\Phi_{e\ \max}(J)$ in function of the applied current J, but as long as this is understood, there is no need to do it explicitly. The definition of $J_{\max}$ takes for granted that transitions between different phase states are possible, as discussed in Ref. [3] and [4]. However, for the system to exhibit always the critical current given by Eq. (18), the transitions should occur always at the crossing points of relevant currents $J^{\langle\widehat{m}\rangle}$, at least in the envelope region.

The transitions between different phase states of a junction must occur via an intermediate normal (resistive) state of the weakest junction in the relevant array [3]. While it can be imagined that a spontaneous transition from a metastable to stable state could occur if these states have the same stationary energies, currents and fluxes (several such triple points can be observed in Fig. 4), nevertheless in general we must associate the transitions with changes in current and flux bias conditions, which threaten to drive the system permanently normal if it does not change its phase state.

In the presence of a constant current bias the transitions will be enabled whenever $J^{(\widehat{m})}(\Phi_e)$ descends below the bias value. If the bias current J exceeds I_{max}, the system can always leave superconducting state exhibiting the envelope value of the critical current. This observation might be helpful in the interpretation of experimental data on magnetoresistance of high-T_c materials [9]. However, it must be observed that the current envelope does not wholly coincide with the energy envelope.

In Ref. [4] the system's evolution in varying external flux was assumed to be governed by the following rules:

1. When two states have equal stationary energies, the system makes a transition to the stable state. If both states are stable, the transition is to the state with negative energy slope with respect to flux change.

2. When the evolution leads beyond a phase vortex limit, the system makes a transition to a state of lower energy.

Application of these rules leads generally to hysteretic system behavior, dependent on its past.

Although plausible, the above rules cannot be considered as strict ones. The response of the system to external flux changes must be determined by its dynamic properties. The foregoing remarks could be considered even as pure speculation if the experiments of Fulton, Dunkleberger and Dynes [7] on highly inductive two-junction interferometers have not put into evidence the phenomenon of multiple critical currents, and have not shown that in dynamical situations the equilibrium currents below the envelope can take on the role of critical currents.

The envelopes shown in Fig. 4 exhibit the effect of "spurious" or "secondary" modulation. The combination of this effect and that of hysteretic multiple critical currents was possibly observed in some high-T_c d.c. SQUID measurements. The same combination might be also responsible for the rather poor fit of experimental and theoretical data in experiments on microwave emission from high-T_c thin films [2], where only parallel arrays of junctions were used in the theoretical interpretation. Let us also observe that the crossing energy levels provide a set of two energy wells required by the two-level fluctuator model of random telegraph noise observed in high-T_c thin films [9].

4. Conclusions

In conclusion, we have shown that stationary properties of a generalized superconducting interferometer, comprising series as well as parallel Josephson junctions, can be derived from the potential energy of the system constituted by the interferometer, its current source and external magnetic flux. In particular, we have shown that critical current of the interferometer corresponds to local extremum of this energy and we have provided analytical tools which, supplemented by numerical methods, can be used not only to evaluate this current but also to find whether the corresponding energy extremum is a minimum or a maximum.

Acknowledgments

Many stimulating discussions with J. Zagrodziński are gratefully acknowledged. The author wishes also to thank Z. Potocki for his help in designing Fig. 1.

References

[1] P. Bernstein, S. Lamarti, J. Bok, *Solid State Commun.* **75**, 587 (1990).
[2] G. Jung, J. Konopka, *Europhys. Lett.* **10**, 183 (1989).
[3] S.J. Lewandowski, *Phys. Rev. B* **43**, 7776 (1991).
[4] S.J. Lewandowski, *Phys. Rev. B*, in press.
[5] M. Klein, A. Mukherjee, *Appl. Phys. Lett.* **40**, 744 (1982).
[6] J. Pełka, J. Zagrodziński, *Physica B* **154**, 4573 (1989).
[7] T.A. Fulton, L.N. Dunkleberger, R.C. Dynes, *Phys. Rev. B* **6**, 858 (1972).
[8] Won-Tien Tsang, T. Van Duzer, *J. Appl. Phys.* **46**, 4573 (1975).
[9] G. Jung, M. Bonaldi, S. Vitale, J. Konopka, *J. Appl. Phys,* **70**,5440 (1991).